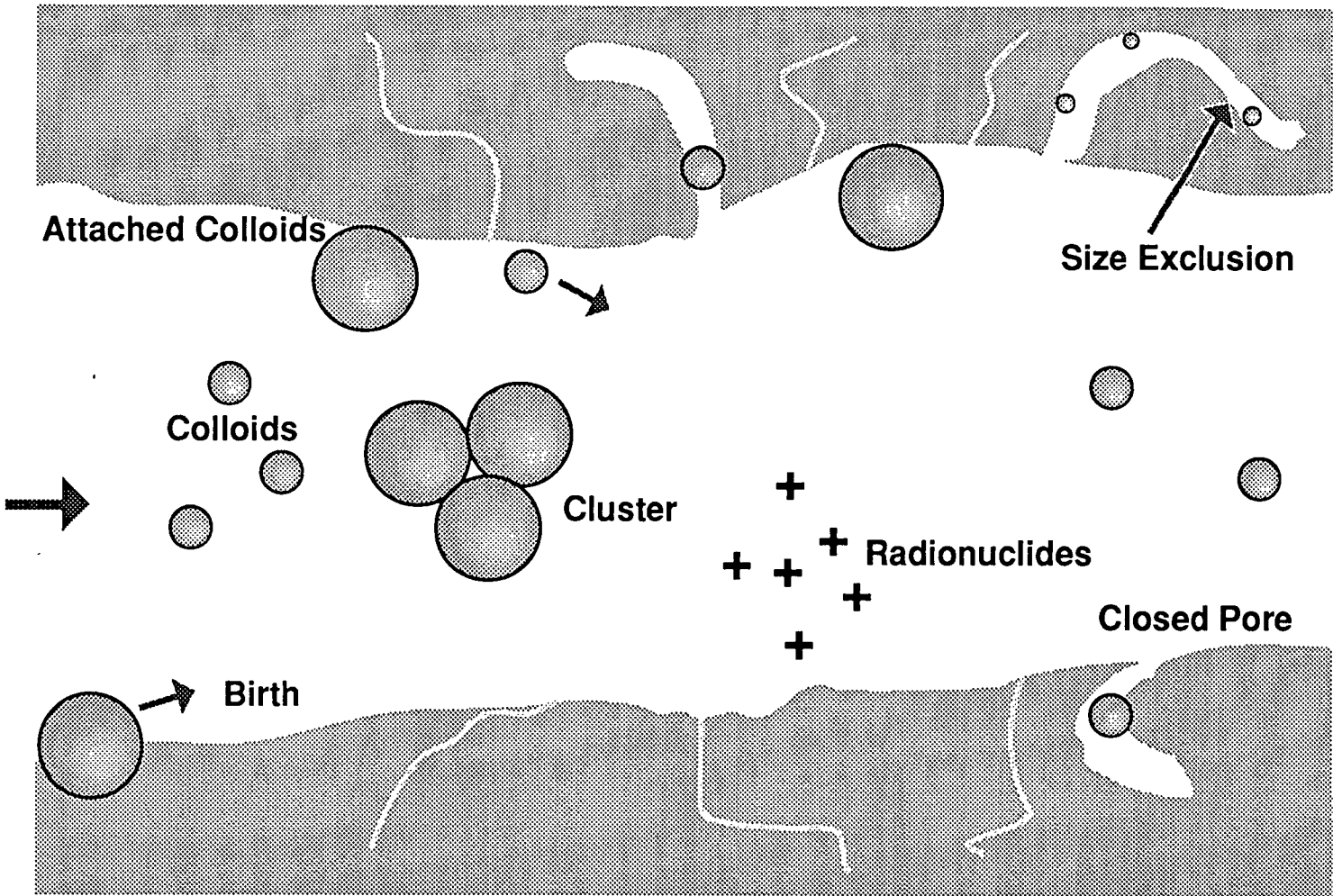


Colloid Formation, Stability, and Transport
“Review of Existing Information”

I. Triay and S. Levy
LANL

Colloid Processes

Rock Matrix



Rock Matrix

Mathematical Description of Colloid Processes

$$\frac{d \{ d[\text{coll}] \cdot d\Phi^{-1} \}}{dt} = P_{(\text{ag})\Phi} + P_{(\text{dg})\Phi} + P_{(\text{er})\Phi} + D_{(\text{dg})\Phi} + D_{(\text{ag})\Phi} + D_{(\text{at})\Phi}$$

The production rates ($P > 0$) for sizes ranging from Φ to $\Phi + d\Phi$ are:

$P_{(\text{ag})\Phi}$ = the aggregation rate from smaller colloids or soluble species

$P_{(\text{dg})\Phi}$ = the disaggregation rate from larger colloids or suspended particles

$P_{(\text{er})\Phi}$ = the erosion rate

The disappearance rates ($D < 0$) for sizes ranging from Φ to $\Phi + d\Phi$ are:

$D_{(\text{dg})\Phi}$ = the disaggregation rate toward smaller colloids or soluble species

$D_{(\text{ag})\Phi}$ = the aggregation rate toward larger colloids or suspended particles

$D_{(\text{at})\Phi}$ = the attachment rate

Colloid Generation

Primary Generation (from erosion)

$$\frac{d[\text{coll}]}{d\Phi} = A \cdot \Phi^{-b}$$

[coll] is colloid concentration, in particles/ml

Φ is size, in nm

A and b are constants

Crystalline Reference Water:

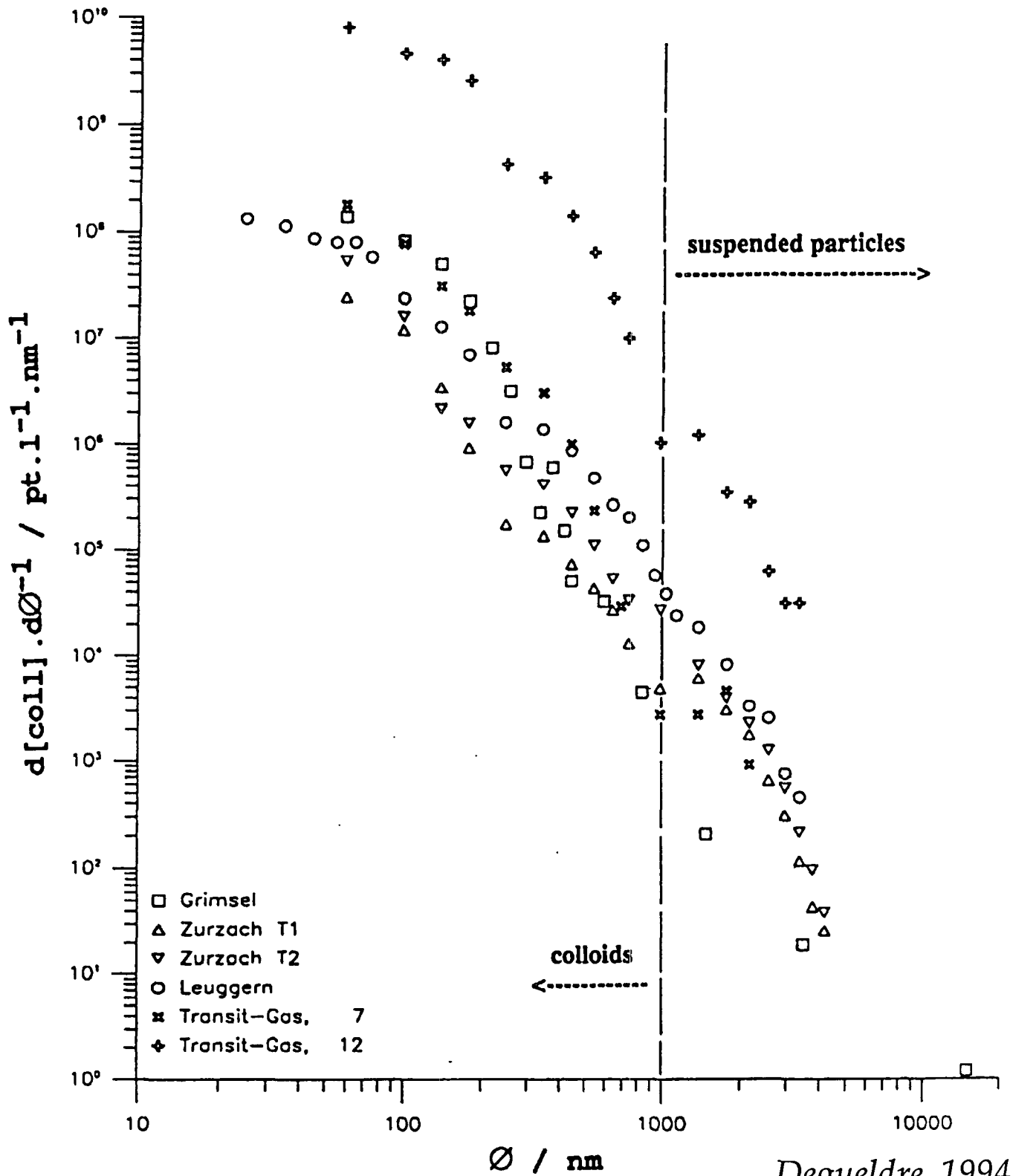
$$\frac{d[\text{coll}]}{d\Phi} = 10^{10.5} \cdot \Phi^{-3}$$

$$[\text{coll}] = 10^{10} \cdot \{\Phi_{(\text{min})}^{-2} - \Phi_{(\text{max})}^{-2}\}$$

≤ 100 ng/ml for sizes in the 10 to 1,000 nm range

Degueldre, 1994

Colloid Size Distributions in Alpine Waters



Colloid Population Stability *Degueldre, 1994*

$$\frac{d \{d[\text{coll}] \cdot d\Phi^{-1}\}}{dt} = P_{(\text{ag})\Phi} + D_{(\text{ag})\Phi} \quad \text{Smoluchowski, 1917}$$

Aggregation for a monodispersed population of spherical colloids

$$\frac{d[\text{coll}]}{dt} = \frac{-4 a k_B T [\text{coll}]^2}{3 \nu} \quad \text{Mills and Liu, 1991}$$

$$t_{1/2} = \frac{3 \nu}{4 a k_B T [\text{coll}]_0}$$

ν = viscosity

k_B = Boltzmann's Constant

T = temperature

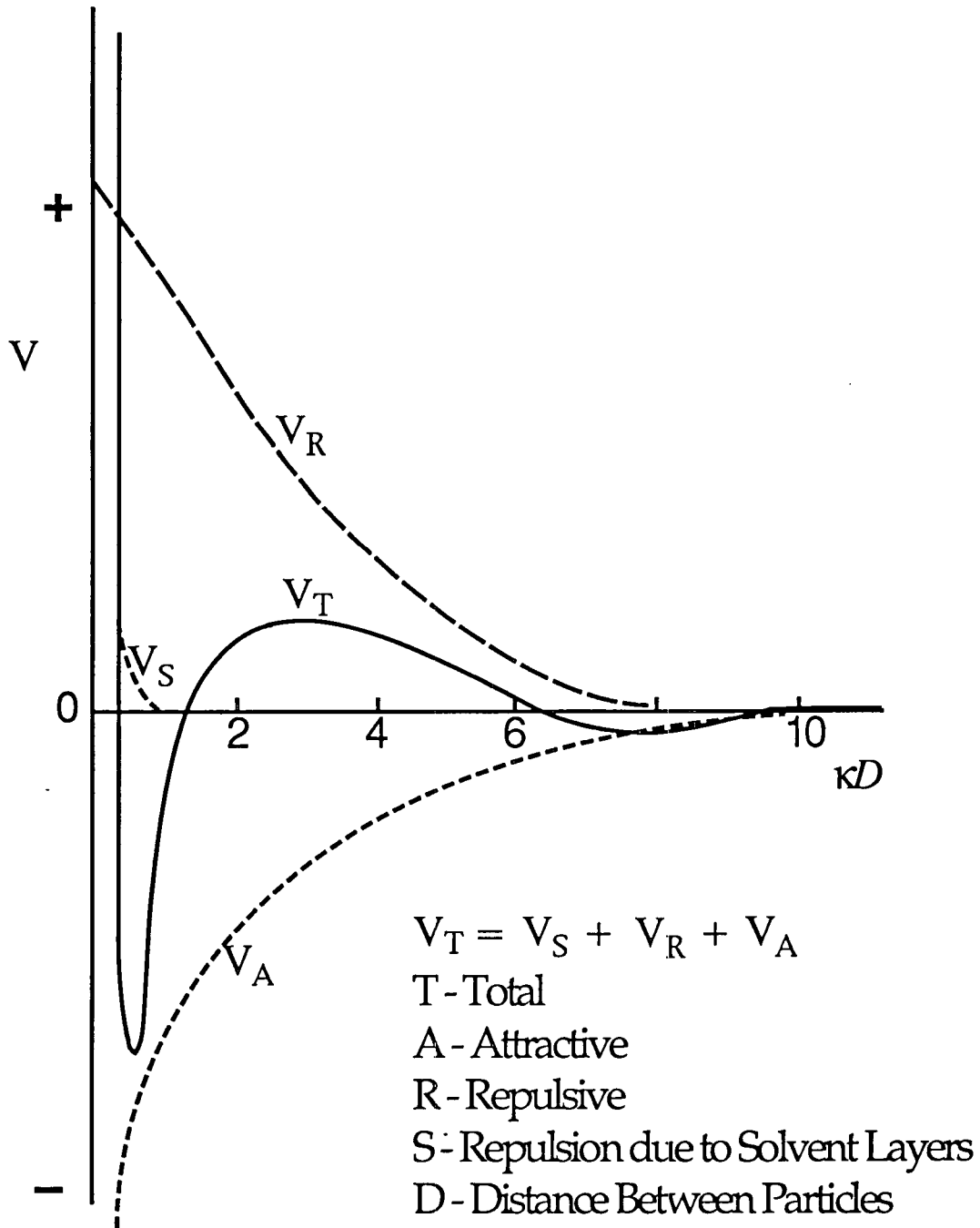
a = attachment factor

Increasing T from 298 to 373 °K and Decreasing ν from 0.9 to 0.3 cP,

Causes $t_{1/2}$ to Decrease by a factor of 4

Increasing $[\text{Na}]$ from 5×10^{-3} to 1×10^{-2} M, Causes $t_{1/2}$ to Decrease by a factor of 25

Potential Energy of Interaction



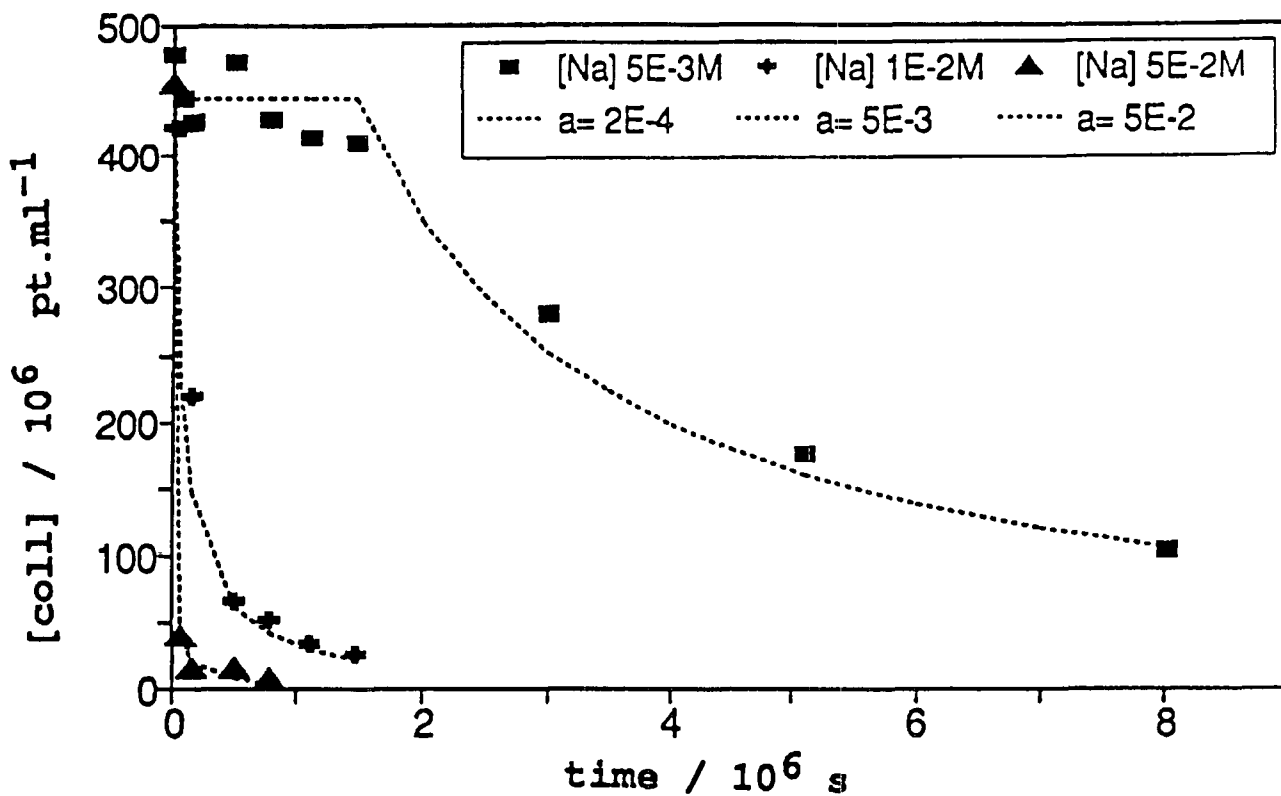
Hunter, 1991

Schulze - Hardy Rule

- electrolyte concentration at which hydrophobic colloid can be completely destabilized depends on the valency of the electrolyte
- critical coagulation concentration ($c \cdot c \cdot c$) corresponds to zero interaction energy and force in DLVO
- $c \cdot c \cdot c \propto \frac{1}{z^6}$ (z is electrolyte charge)
- increases of attachment factor occur at concentrations greater than 10^{-2} M for alkali cations and greater than 10^{-4} M for alkaline earth cations (*Degueldre, 1994*)
- attachment factor must be measured (*Grauer, 1990*)

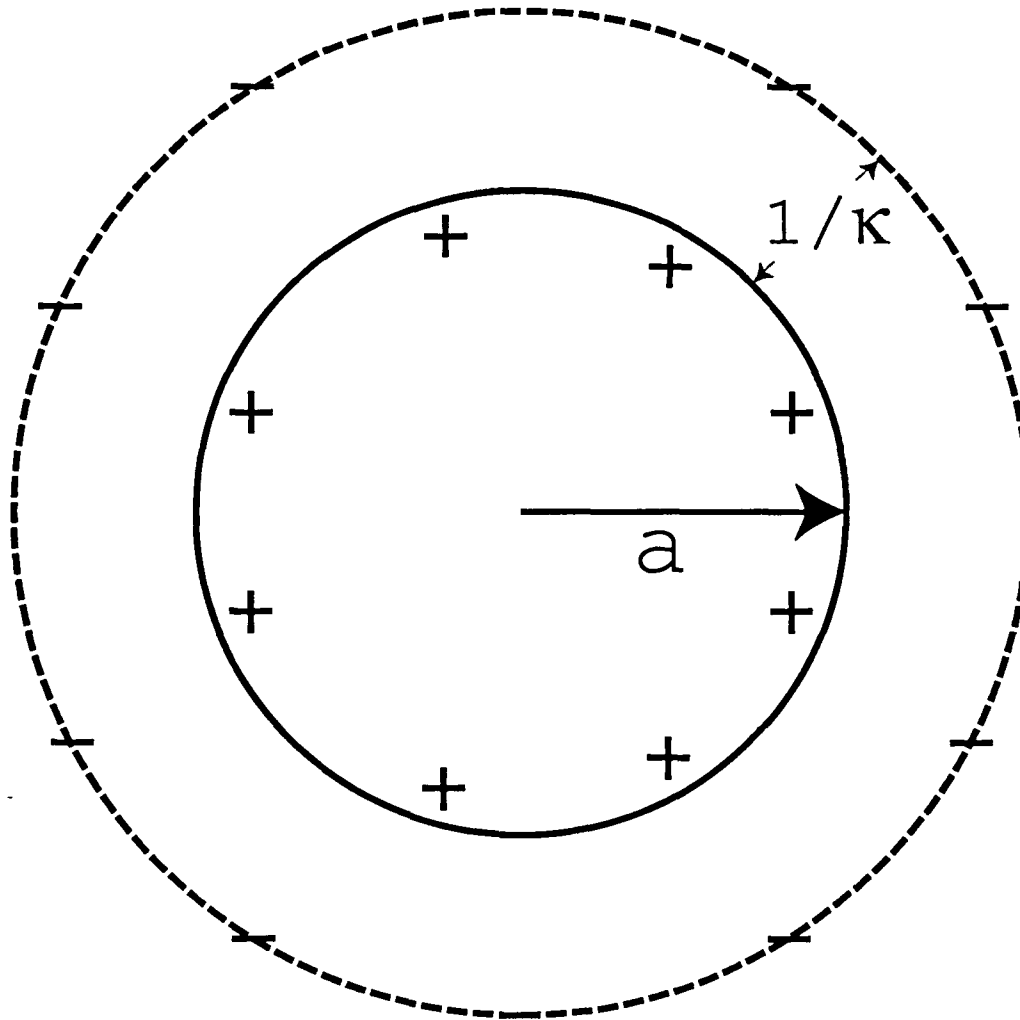
Effect of Na Concentration on Montmorillonite Colloids Stability

Colloids are ≥ 100 nm, pH = 8



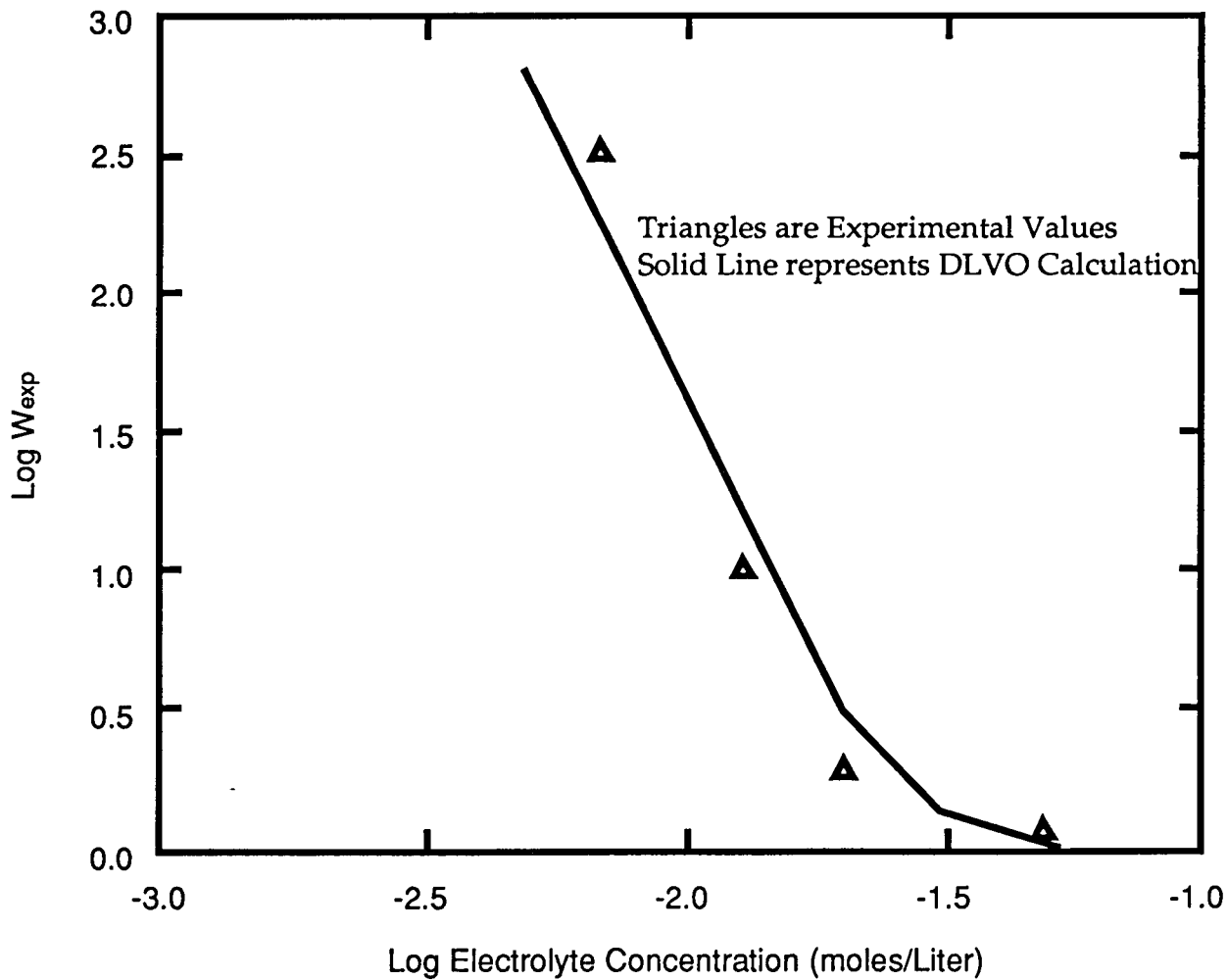
Degueldre, 1994

Distribution of Charge Around a Particle



Hunter, 1991

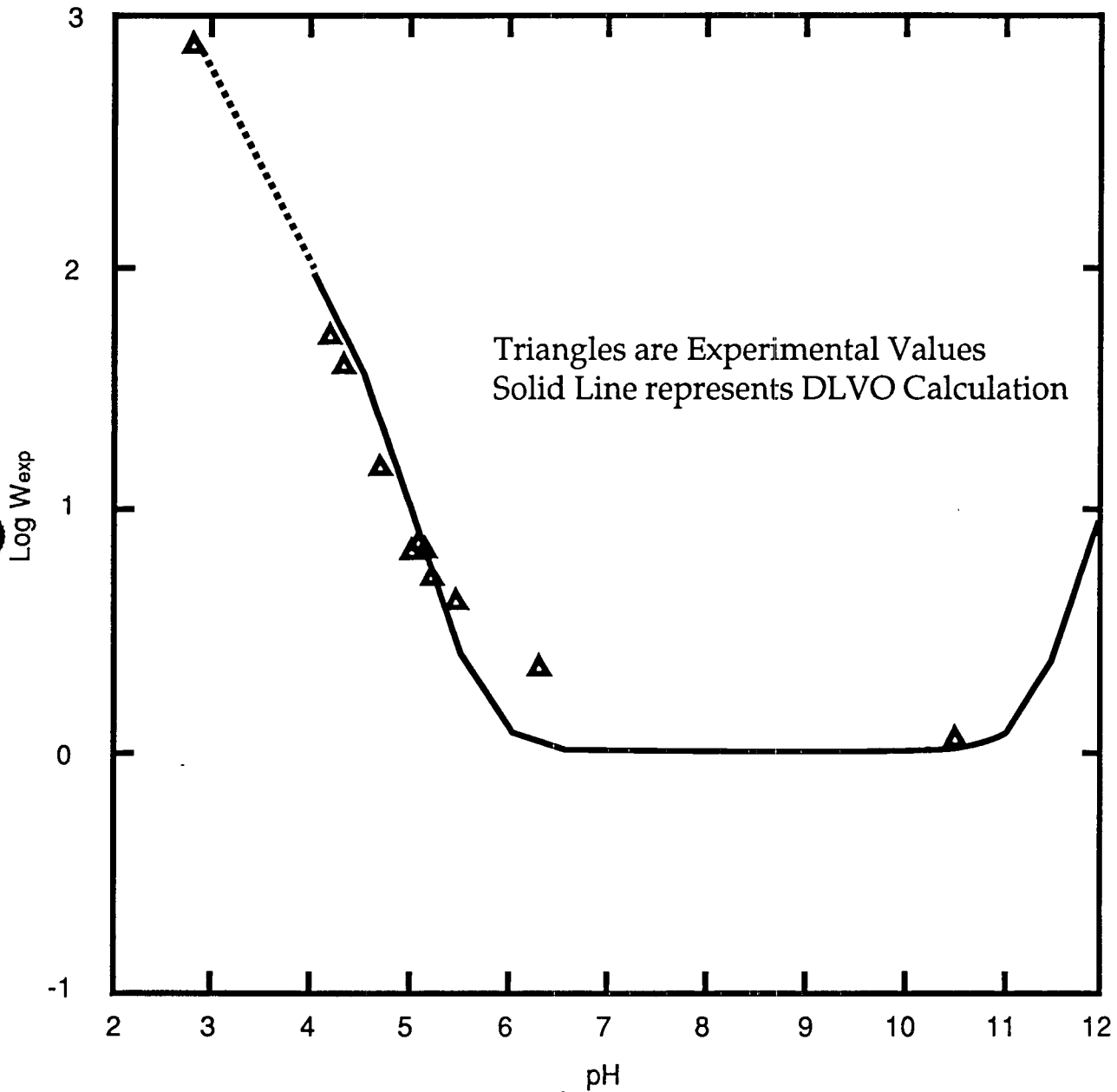
Stability of a Hematite Suspension as a Function of Na Concentration at pH 10.5



W represents how stable a colloidal suspension is
with respect to Diffusion-Controlled Aggregation

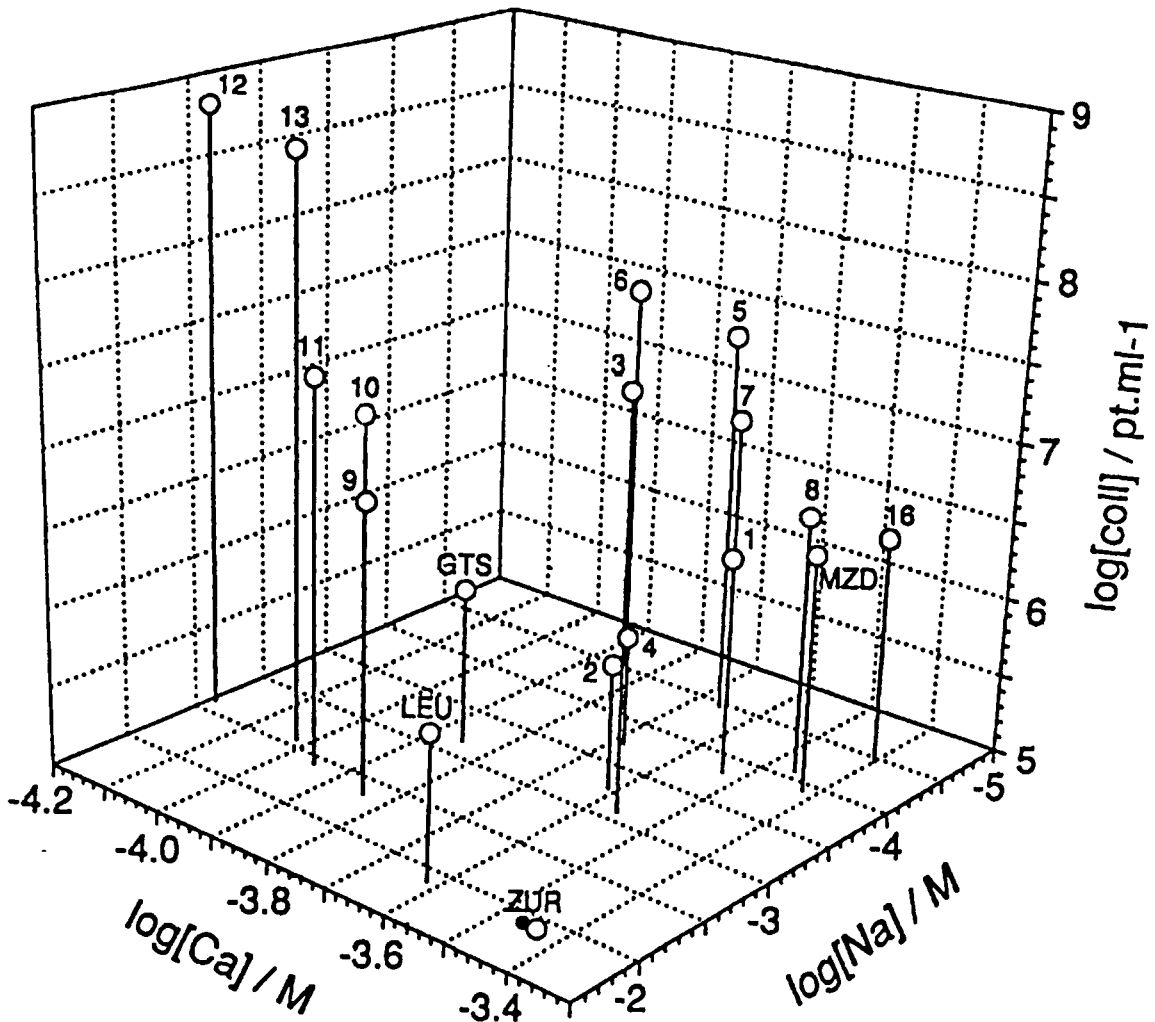
Liang, 1988

Stability of a Hematite Suspension as a Function of pH at $I = 0.05M$



W represents how stable a colloidal suspension is with respect to Diffusion-Controlled Aggregation

Groundwater Colloid Concentration in the Size Range from 100 to 1,000 nm as a function of Na and Ca Concentration



Degueldre, 1994

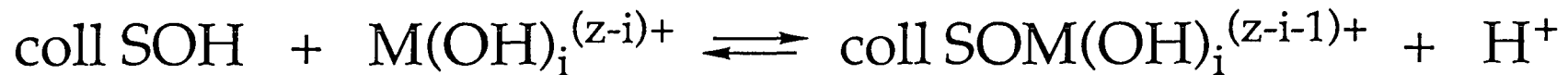
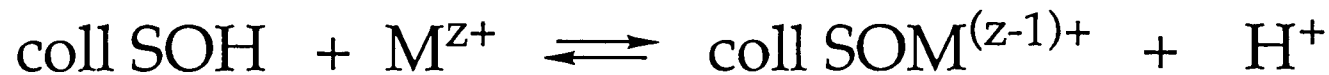
Colloid concentration in J-13 is 10^6 particles/ml
at $[\text{Na}] = 2 \times 10^{-3} \text{ M}$ and $[\text{Ca}] = 3 \times 10^{-4} \text{ M}$

Triay, et al. 1994

Radionuclide Sorption onto Colloids

$$R_p = \frac{[M]_{\text{coll}}}{[M]_{\text{soluble}}} \cdot \frac{1}{[\overline{\text{coll}}]}$$

$[\overline{\text{coll}}]$ in g/ml



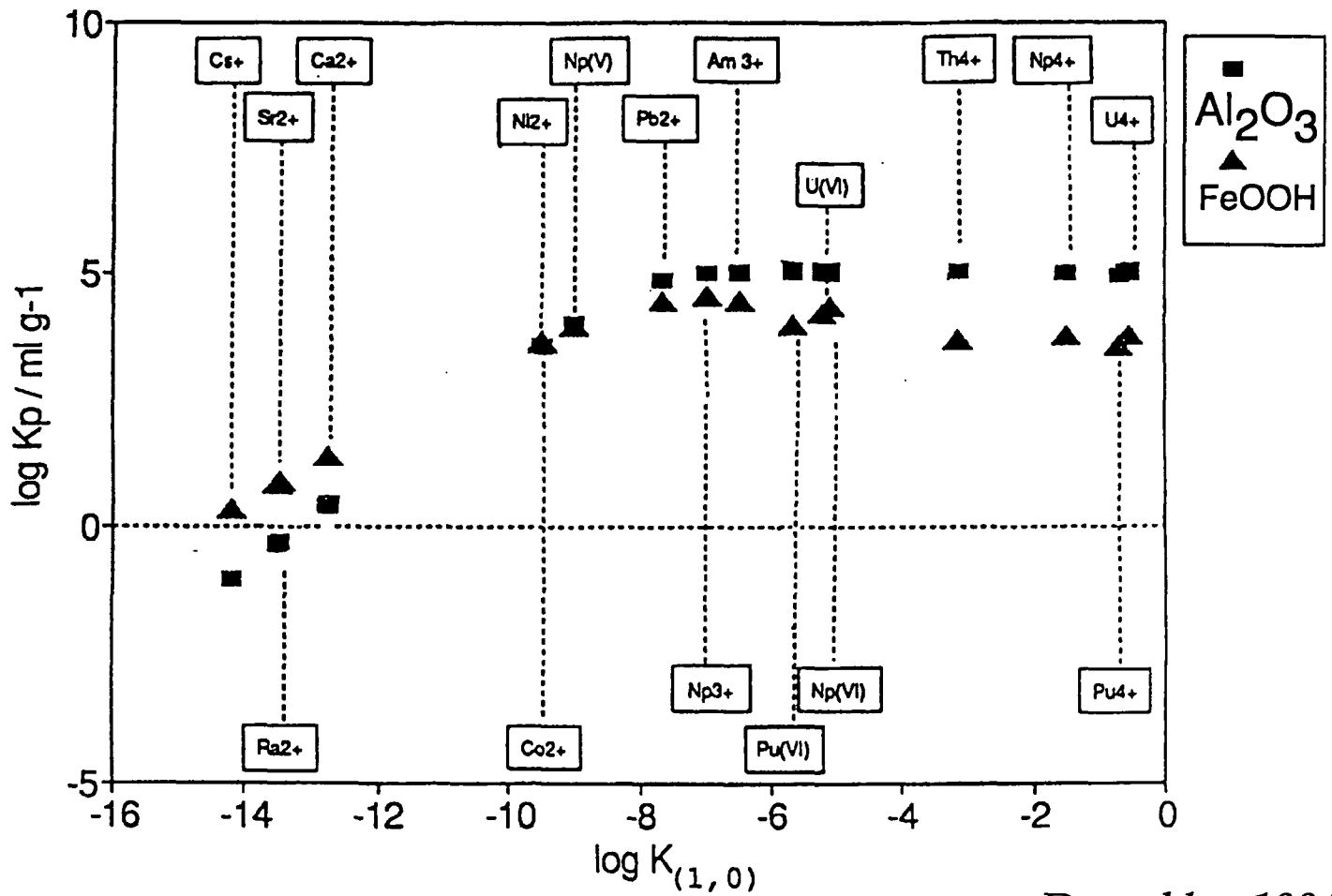
$$K_p = \frac{\{ [\text{SOM}^{(z-1)+}] + \Sigma [\text{SOM}(\text{OH})_i^{(z-i-1)+}] \}}{\{ [M^{z+}] + \Sigma [M(\text{OH})_i^{(z-i)+}] \}} \cdot \frac{1}{[\overline{\text{coll}}]}$$



Degueldre, 1994

Correlation Between K_p (for Radionuclide Sorption at pH 8) and First Hydrolysis Constant

assuming $\Phi = 200 \text{ nm}$, $\rho = 2 \text{ g/cm}^3$, and Site Density = 3 sites/nm^2



Degueldre, 1994

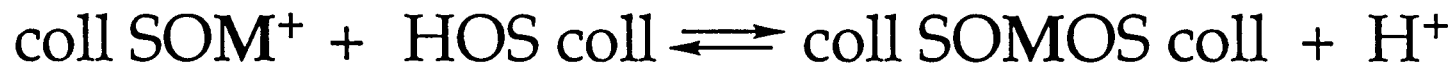
Radionuclide Sorption as a Function of Colloid Type

Colloid Type	Species	[M] (mol/l)	pH	R _p (ml/g)	K _p (ml/g)
Quartz	Am(III)	8.0×10^{-10}	8	2×10^4	---
Amorphous silica (20 nm)	Am(III)	8.0×10^{-10}	8	3×10^6	---
Montmorillonite (200 nm)	Pb(II)	2.8×10^{-9}	8	5×10^5	2×10^5
	Ni(II)	2.0×10^{-10}	8	5×10^3	10^3
	Am(III)	8.0×10^{-10}	8	3×10^5	5×10^4
Illite (200 nm)	Am(III)	8.0×10^{-10}	8	3×10^5	5×10^4

Degueldre, 1994

Radionuclide Sorption Irreversibility

- Sorption followed by colloid aggregation



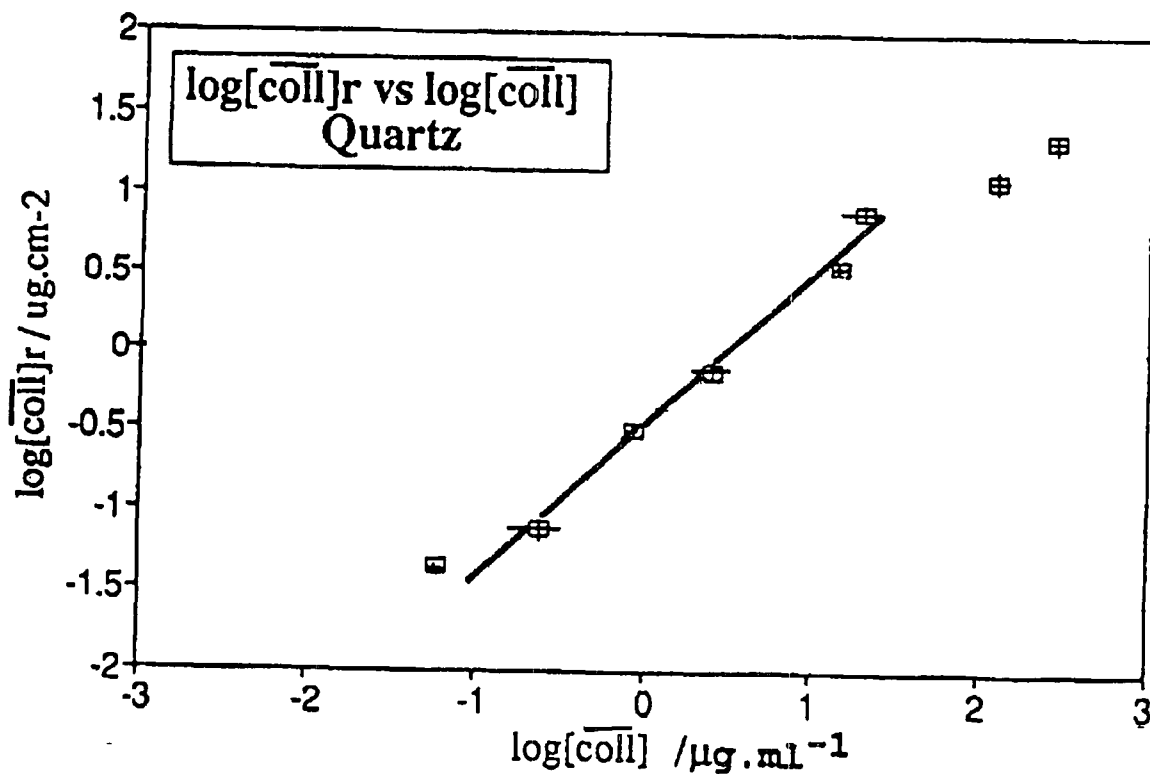
- Sorption followed by coating
- Sorption by coprecipitation
- Sorption into internal sites (e.g., in clay interlayer)

If Reversible Sorption,

- Sorption onto colloids is negligible compared to sorption onto rock (rock surface much larger than surface of colloids for low colloid concentration)

Degueldre, 1994

Montmorillonite Colloids Attachment to Quartz at pH = 8, I = 10⁻² M, Measured after 4-6 hr



$\overline{[\text{coll}]}_r$ is concentration of colloid reversibly attached per unit area of rock

$\overline{[\text{coll}]}$ is concentration of colloids in suspension

Degueldre, 1994

Conclusions and Summary of Data Needs for the Yucca Mountain Project

Triay et al., 1994

- A sensitivity analysis study to assess important parameters for colloid-facilitated radionuclide transport can be performed

Assumptions:

- #1 colloids generated are clays, silica, and iron oxides
 - #2 negligible amount of TOC in groundwaters
 - #3 determine stable colloid population (based on available stability diagrams, groundwater chemistry, and expected T)
 - #4 irreversible sorption of radionuclides onto colloids
 - #5 calculate K_p based on K_d (or use K_p from the literature $\sim 3 \times 10^4$ ml/g for the tri and tetravalent actinide species)
 - #6 no attachment of colloids onto fracture walls
 - #7 colloids excluded from tuff pores due to size and charge
- Experimentally determine type of colloids generated from spent fuel (to address #1)
 - Study Yucca Mountain as its own analog (to address #1)
 - Experimentally determine TOC in groundwaters on line (to address #2)

Conclusions and Summary of Data Needs for the Yucca Mountain Project (continued)

Triay et al., 1994

- Experimentally determine stability diagram for silica (to address #3)
- Experimentally determine colloid population in groundwaters and size distributions using off-line particle counting techniques (to address #3 and #5, since K_p depends on particle size)
- Experimentally determine selected K_p values for clay and silica using likely groundwaters (to address #5)
Note: K_p values can already be calculated for iron oxides based on surface complexation studies with U and Np in the presence of CO_2
- Experimentally determine degree of colloid attachment to fracture walls using fractured tuff columns (to address #6)
- Perform transport field experiment (under saturated conditions) in C Wells (to address #7)
- Perform transport field experiment (under unsaturated conditions) using nuclear test at the NTS as a source term (to address #7)

ACTINIDE SORPTION BY COLLOIDAL SILICA

Experimental coprecipitation of dissolved uranium and silica gel:

[U]dried silica gel/[U]solution = 400 to 1000

pH = 7.0 to 8.5

T = 25 to 80°C

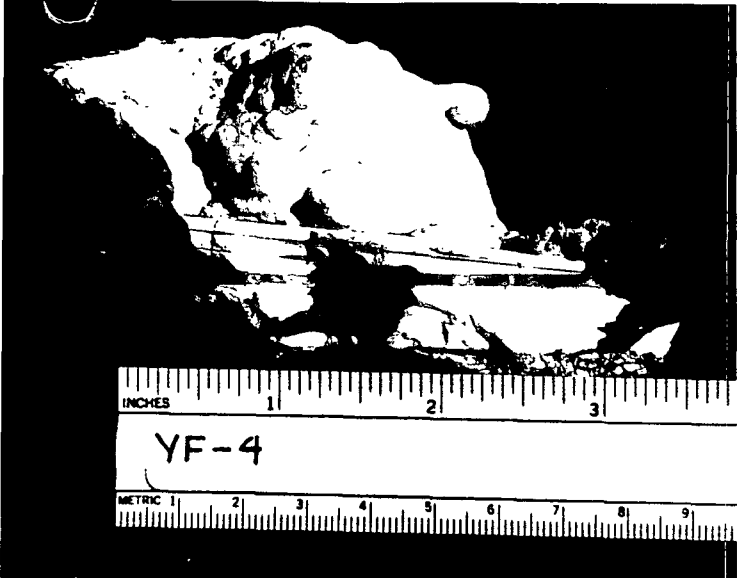
Studies of natural materials:

- post-depositional U immobility within opal
- no data on surface adsorption by opal deposits
- variations in U content correlate with differences in silica crystallinity

(Zielinski, 1982)

GEOLOGIC EVIDENCE OF COLLOID TRANSPORT

- **Yucca Mountain** as natural analog
- **Evidence:** deposits of crystallized gels, settled and adsorbed aggregates of colloids, polymers, and monomers.

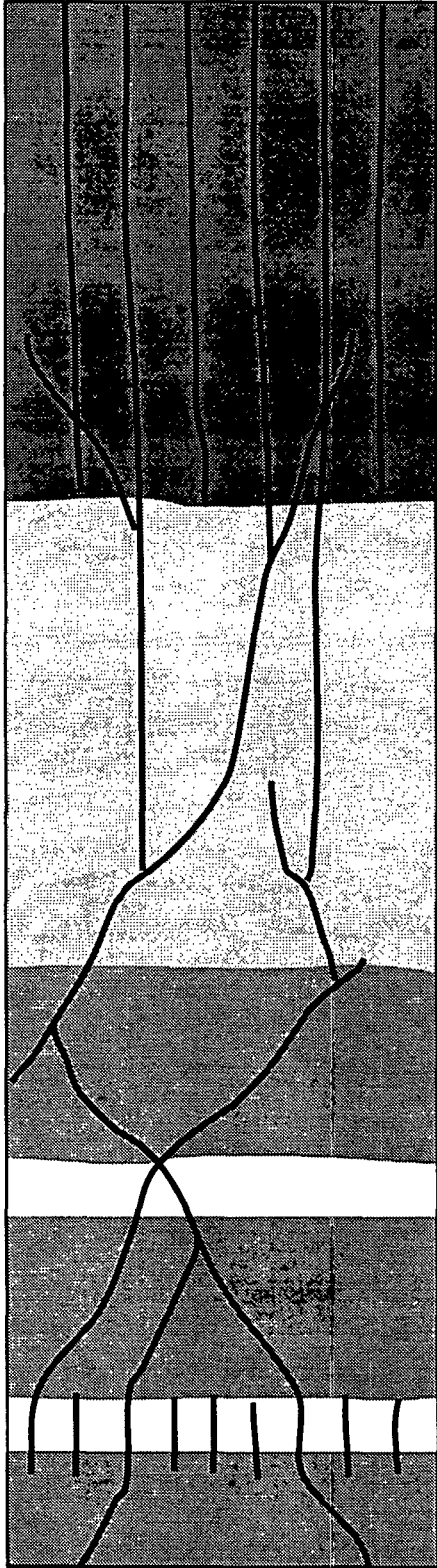


Devitrification cavity in lower Topopah Spring vitrophyre, with silica fillings.

The next vuegraph (not included) shows the same cavity with silica fillings fluorescing under short-wave ultraviolet light due to the uranium content of the silica.

ANALOG ENVIRONMENT

- Hydrothermal conditions — cooling pyroclastic deposit
- Localized, transient fluid flow in the unsaturated zone
- Pyroclastic rocks as sources of abundant colloids:
 - silica (opal-A, opal-CT, cristobalite, quartz)
 - aluminosilicates (smectite, zeolites)
- Total path length places upper bound on colloid transport distance



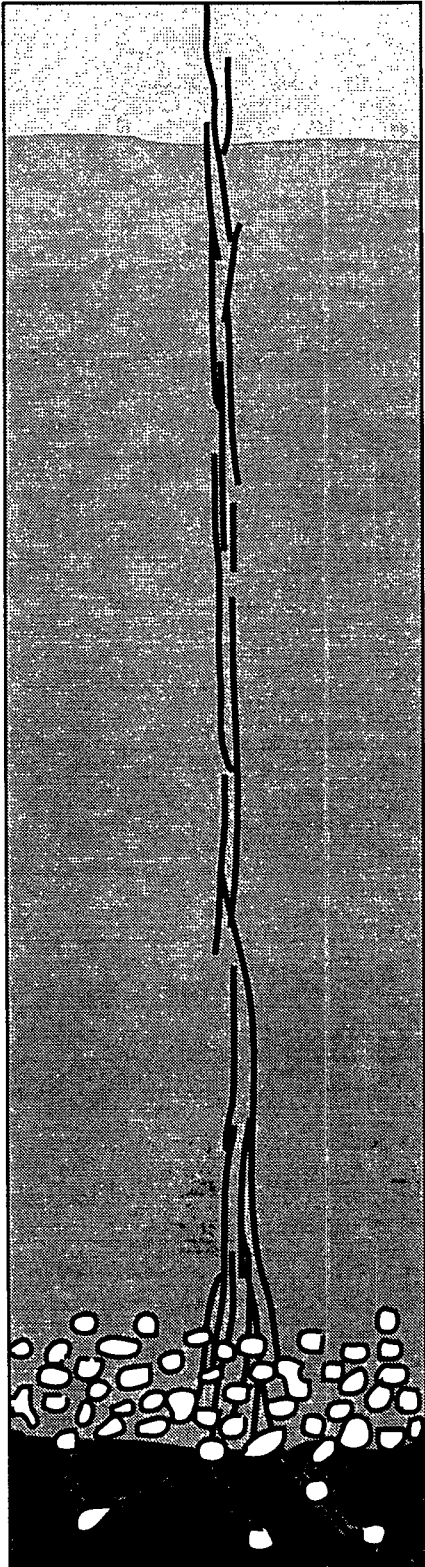
SOUTHEAST YUCCA MOUNTAIN (HARPER VALLEY)

Affected rock units: middle to lower Tiva Canyon tuff and underlying bedded tuffs.

Pathway: Columnar joints in densely welded tuff communicate downward with more irregular vertical fractures in moderately welded tuff and bedded tuffs.

Colloidal material: silica

Path length: ~15 m



NORTHEAST YUCCA MOUNTAIN

Affected rock units: upper Topopah Spring tuff to lower Topopah Spring vitrophyre.

Pathway: vertical fracture zone from top of Topopah Spring tuff terminates in top of vitrophyre, but communicates with fractures connecting devitrification cavities in upper part of vitrophyre

Colloidal material: silica

Path length: ~90 m

LIMITATIONS ON TRANSPORT

Chemical processes and their consequences

agglomeration

adsorption

crystallization

settling

evaporation

Continuity and connectivity of fractures

ISSUES OF TIMING AND KINETICS

What will be the condition of colloidal silica in the repository when canister leakage occurs?

Will adsorbed actinides be remobilized if silica recrystallization occurs?